




OPEN

Early functional connectivity alterations in contralesional motor networks influence outcome after severe stroke: a preliminary analysis

Hanna Braaß^{1,2}, Lily Gutgesell^{1,2}, Winifried Backhaus¹, Focko L. Higgen¹, Fanny Quandt¹, Chi-un Choe¹, Christian Gerloff¹ & Robert Schulz¹

Connectivity studies have significantly extended the knowledge on motor network alterations after stroke. Compared to interhemispheric or ipsilesional networks, changes in the contralesional hemisphere are poorly understood. Data obtained in the acute stage after stroke and in severely impaired patients are remarkably limited. This exploratory, preliminary study aimed to investigate early functional connectivity changes of the contralesional parieto-frontal motor network and their relevance for the functional outcome after severe motor stroke. Resting-state functional imaging data were acquired in 19 patients within the first 2 weeks after severe stroke. Nineteen healthy participants served as a control group. Functional connectivity was calculated from five key motor areas of the parieto-frontal network on the contralesional hemisphere as seed regions and compared between the groups. Connections exhibiting stroke-related alterations were correlated with clinical follow-up data obtained after 3–6 months. The main finding was an increase in coupling strength between the contralesional supplementary motor area and the sensorimotor cortex. This increase was linked to persistent clinical deficits at follow-up. Thus, an upregulation in contralesional motor network connectivity might be an early pattern in severely impaired stroke patients. It might carry relevant information regarding the outcome which adds to the current concepts of brain network alterations and recovery processes after severe stroke.

Magnetic resonance imaging (MRI) based connectivity analyses have significantly contributed to our present understanding of how functional brain networks are affected by acute stroke lesions and how these changes are associated with residual motor function and recovery processes¹. Most evidence has been accumulated for networks connecting sensorimotor cortices of both hemispheres with preserved or increased interhemispheric connectivity being positively related to favorable outcomes^{2–5}. Compared to interhemispheric connectivity, there are few data to support the view that alterations in intrahemispheric coupling profiles within the ipsilesional^{6–9} and especially the contralesional hemisphere^{10–13} might explain inter-subject variability in motor functions or recovery after stroke. In addition to such analyses of connection strengths within rather small, selected networks, graph-theoretical analyses on more complex, large-scale networks have provided complementing insights. For instance, they have shown that network topography, assessed by modularity, a measure of integration within and segregation between brain systems, also shows significant alterations after stroke, not only in the ipsilesional but also in the contralesional hemisphere^{14,15}. Such data have promoted current concepts how interhemispheric and intrahemispheric network alterations, along with their topographic implication on network architecture, can explain deficits and recovery after stroke. Nevertheless, MRI data from clinical cohorts particularly investigating the contralesional coupling changes obtained in the acute to the early subacute stage are remarkably scarce but functional^{16–18} and structural MRI imaging^{19–21}, and non-invasive brain stimulation^{22–24} have convergingly indicated that the sensorimotor parieto-frontal network of the contralesional hemisphere is involved in recovery after stroke, with greater importance in more severely impaired patients.

¹Department of Neurology, University Medical Center Hamburg-Eppendorf, Martinistraße 52, 20246 Hamburg, Germany. ²These authors contributed equally: Hanna Braaß and Lily Gutgesell. ✉email: h.braass@uke.de

The study aimed to investigate early functional network changes with a focus on key areas of the contralateral parieto-frontal motor network and their relevance for the functional outcome after severe motor stroke. Structural and resting-state functional MRI data, obtained within the first 2 weeks after severe stroke, were re-analyzed from a previously published prospective cohort study of severely impaired acute stroke patients and integrated with clinical follow-up data of the late subacute stage of recovery after 3–6 months⁶. In the original analysis of that study, we had focused on the ipsilesional parieto-frontal motor network while contralateral network alterations and their importance for functional outcome were not considered⁶. In the present report, we now used a seed-based approach to assess contralateral resting-state functional connectivity (FC) involving five key motor areas, that are the primary motor cortex (M1), ventral premotor cortex (PMV), supplementary motor area (SMA), and anterior and caudal intraparietal sulcus (AIPS, CIPS). We hypothesized that stroke patients would show (1) significant alterations in contralateral inter-regional FC early after stroke, and (2) a significant association between FC estimates and subsequent recovery.

Results

Demographics and clinical characteristics. Nineteen patients (12 females and 7 males, all right-handed, aged 73.8 ± 5.8 years) and 19 healthy controls (12 females and 7 males, all right-handed, aged 75.3 ± 7.5 years) were included in the analysis. A topographic map of the distribution of stroke lesions is shown in Fig. 1. Clinical characteristics are given in Supplementary Table 1. Early clinical examination was conducted on average on day 7 (mode day 5, range 3–13) after stroke. Late sub-acute stage follow-up data ($T_{2/3}$) were derived from clinical examination after 128 days on average (mode 89, range 86–217). Linear mixed-effects models evidenced significant functional improvements over time in ‘early rehabilitation’ Barthel Index (BI)²⁵, Fugl Meyer Assessment of the upper extremity (UEFM), modified Rankin Scale (MRS), and National Institutes of Health Stroke Scale (NIHSS) (all $P < 0.001$, details are shown in⁶).

Alterations in contralateral functional connectivity after stroke. Seed-based whole brain analyses revealed FC alterations between contralateral seed areas M1, PMV, SMA, and CIPS and multiple brain regions of both hemispheres compared to healthy controls in the acute phase after stroke. No significant differences were found for AIPS. Table 1 shows the group differences for contralateral FC between stroke patients and controls and Fig. 2 illustrates the topography of contralateral clusters exhibiting FC alterations after stroke. For M1, we detected an increase in FC with precuneus, cingulate gyrus, SMA, and precentral gyrus (region of the dorsal premotor cortex). SMA was found to be more strongly connected to the sensorimotor cortex (SMC), more precisely, the peak coordinate of the SMC cluster is located in the sulcus centralis between contralateral precentral and postcentral gyrus. Increases in FC were also detected for SMA and frontal pole, middle frontal gyrus (MFG), lateral occipital cortex, and precuneus. PMV exhibited stronger FC with frontal pole and MFG, and CIPS was more strongly coupled with a cluster localized in precuneus and cingulate cortex.

Associations between altered contralateral functional connectivity and future persistent deficits after stroke. Linear models were fitted to relate FC values in the acute phase to clinical outcome after 3–6 months, operationalized by means of BI, UEFM, MRS and NIHSS (Table 2). The main finding was a consistent association of the FC between contralateral SMA and SMC and clinical outcome and upper limb function. An early increase in FC was linked to lower scores in BI ($P = 0.002$), in UEFM ($P = 0.018$) and higher scores in MRS ($P = 0.024$) at follow-up. For NIHSS, we observed a compatible statistical trend ($P = 0.067$). Importantly, the association of FC values obtained early after stroke and functional outcome at follow-up was independent from the initial deficit. Notably, there was no correlation between FC values and initial deficits. The addition of SMA-SMC FC to the initial behavioral scores increased the explained variance by 30% in future BI, 24.5% in UEFM, and 22% in MRS, respectively (see Table 3 and Fig. 3 for statistical model results).

Further, FC-outcome associations with the same direction were detected for M1-SMA FC and MRS ($P = 0.038$), PMV-MFG FC and MRS ($P = 0.038$), and CIPS-Precuneus/Cingulate Gyrus FC and NIHSS ($P = 0.047$) (Table 3).

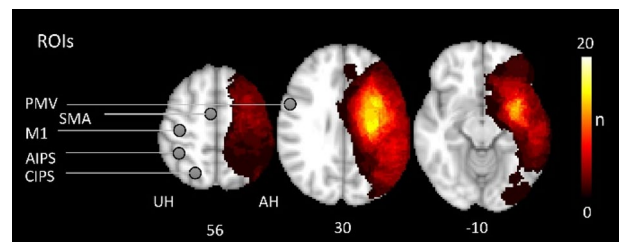


Figure 1. Stroke lesions and motor network regions of interest (ROI). All masks of stroke lesions are displayed in the left hemisphere (affected hemisphere, AH), overlaying a T1-weighted template in MNI space (z-coordinates below each slice). The color intensity indicated the number of subjects of whom lesion voxels lay within the colored region. Contralateral motor ROIs (M1, PMV, SMA, AIPS and CIPS) are displayed on the unaffected hemisphere (UH). An additional frequency map of the stroke lesions in the right and left hemisphere can be found in the supplementary material (Supp. Figure 1).

Seed	Region	Cluster	MNI Coord.			Cluster size	P_{FDR}	T
			x	y	z			
M1	Precuneus	1	0	-40	66	590	<0.0001	5.5
	Cingulate gyrus	2	2	-16	42	146	<0.001	4.86
	SMA	3	10	-14	60	55	0.026	4.73
	Precentral gyrus	4	36	-6	52	51	0.029	4.5
PMV	Frontal pole	5	20	56	24	105	0.008	4.51
	Middle frontal gyrus (MFG)	6	42	12	60	58	0.03	5.10
	MFG	7	42	30	20	56	0.033	5.21
SMA	Frontal pole	8	12	44	52	363	<0.0001	5.58
	MFG	9	48	26	46	222	<0.0001	5.27
	Lateral occipital cortex	10	34	-60	28	75	0.013	4.31
	Postcentral/precentral gyrus (SMC)	11	48	-16	58	55	0.025	4.88
	Precuneus	12	6	-64	46	51	0.031	4.58
CIPS	Precuneus/cingulate gyrus	13	8	-50	34	74	0.045	4.54

Table 1. FC changes in the contralesional hemisphere compared to healthy controls. Clusters exhibiting significant increases in patients compared to controls are given with region information, MNI coordinates, cluster sizes, FDR-corrected P and T values. Results are derived from a cluster size threshold of $P < 0.05$ (FDR-corrected) and a voxel threshold of $P < 0.001$ (uncorrected). The Harvard Oxford atlas was used for the region classification.

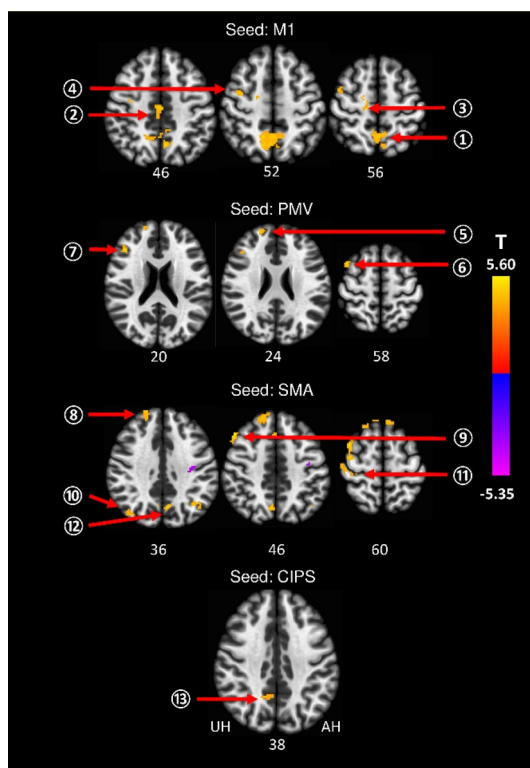


Figure 2. FC changes after stroke from contralesional seed regions compared to healthy controls. Clusters exhibiting significant changes in FC for M1, PMV, SMA and CIPS as contralesional seed regions are superimposed on a standard T1 image in MNI space. T values are color-coded with orange yellow indicating an increase in FC in stroke patients, and blue indicating a decrease in FC (T values were thresholded with a threshold value of $|T| > 3.58$). The numbers of the unaffected (contralesional) hemisphere refer to the cluster IDs used in Table 1. Z-values in MNI space are given below each axial slice. AH affected hemisphere, UH unaffected hemisphere. For details of contralesional clusters, please see Table 1.

Seed	Region	Cluster	BI T _{2/3}		UEFM T _{2/3}		MRS T _{2/3}		NIHSS T _{2/3}	
			Coef.	P _{unc}	Coef.	P _{unc}	Coef.	P _{unc}	Coef.	P _{unc}
M1	Precuneus	1	-96.83	0.13	-50.87	0.34	4.63	0.06	-2.39	0.87
	Cingulate gyrus	2	-19.77	0.63	-12.68	0.70	2.91	0.06	8.25	0.40
	SMA	3	-29.40	0.53	-43.11	0.25	3.63	0.038	8.73	0.59
	Precentral gyrus	4	5.39	0.88	16.31	0.54	2.24	0.12	-9.91	0.44
PMV	Frontal pole	5	-39.96	0.27	-6.29	0.83	2.16	0.12	8.45	0.41
	Middle frontal gyrus (MFG)	6	-55.63	0.56	-41.29	0.54	6.04	0.038	4.40	0.83
	MFG	7	-14.89	0.8	5.15	0.93	1.82	0.46	-8.06	0.55
SMA	Frontal pole	8	-1.76	0.98	46.33	0.27	1.99	0.31	-3.71	0.81
	Middle frontal gyrus (MFG)	9	-50.40	0.27	-5.19	0.91	2.6	0.20	-6.53	0.63
	Lateral occipital cortex	10	87.51	0.20	49.62	0.34	2.87	0.40	-18.17	0.30
	Postcentral/precentral gyrus (SMC)	11	-78.27	0.002	-60.82	0.018	3.08	0.024	13.85	0.067
	Precuneus	12	-36.32	0.37	-23.89	0.48	2.72	0.12	-2.71	0.82
CIPS	Precuneus/Cingulate gyrus	13	-24.69	0.59	-51.16	0.09	2.42	0.17	15.82	0.047

Table 2. Association of contralesional functional connectivity and future persistent deficits. Coefficients are given incl. their *P*-values (uncorrected within models) for contralesional FC (obtained at timepoint T₁) as the main predictor. Results are derived from independent models for the four outcome scores and follow-up timepoint T_{2/3}. Significant findings are highlighted in bold. See Table 3 for further model details for SMA-SMC FC (cluster 11).

Outcome	Predictor	Model summary		
		Coef	P _{unc}	R ²
BI T _{2/3}	SMA—SMC	-78.27	0.0015	0.84
	BI T ₁	1.24	0.0021	
	Age	-2.88	0.0016	
UEFM T _{2/3}	SMA—SMC	-60.82	0.0176	0.78
	UEFM T ₁	0.72	0.0210	
	Age	-1.03	0.155	
MRS T _{2/3}	SMA—SMC	3.08	0.024	0.61
	MRS T ₁	1.42	0.037	
	Age	0.09	0.095	
NIHSS T _{2/3}	SMA—SMC	13.85	0.067	0.55
	NIHSS T ₁	0.37	0.36	
	Age	0.48	0.051	

Table 3. Association of contralesional SMA-SMC FC and future persistent deficits. Coefficients are given incl. their *P*-values (uncorrected within models) for contralesional SMA-SMC FC (cluster 10, obtained at timepoint T₁) as the main predictor for the four outcome scores and follow-up timepoint T_{2/3}. FC-outcome relationships are adjusted for the influence of the initial deficit and age. R² shows multiple R². Significant findings are highlighted in bold.

Discussion

In patients with severe stroke at initial presentation, we found an increase in contralesional functional connectivity between SMA and sensorimotor cortex (SMC). The increase in FC was negatively associated with the extent of persistent deficits at follow-up after 3–6 months, independently of the initial deficits and age.

The present findings of an early increase in contralesional FC is well in line with previous work showing an upregulation in activity in contralesional motor areas including SMA and SMC, particularly in more severely impaired patients with poor motor outcome^{16,17}. For instance, one study in 11 acute stroke patients found a global reduction of task-related activity acutely after stroke followed by increases in ipsilesional and contralesional motor areas within the first 10 days²⁶. Such increases in contralesional activation might persist over time even in well-recovered patients^{27,28}. In contrast, other studies found downregulated activity in contralesional SMA in the chronic stage of recovery^{29,30}. Inter-study variability, e.g., in the level of impairment and time points, leads to a rather complex picture of time- and recovery-dependent changes in brain activation¹⁸. In addition to local activation, stroke also leads to widespread changes in inter-regional connectivity. In fact, most evidence is available for interhemispheric connections and intrahemispheric connections of the ipsilesional hemisphere^{1,6–9}. Data on contralesional coupling dynamics and their importance for recovery are remarkably limited. The situation is

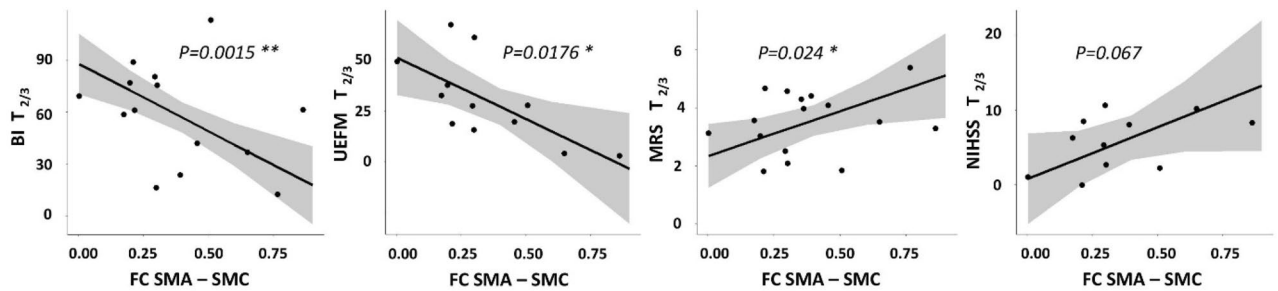


Figure 3. Influence of contralesional FC on future persistent deficits after stroke. Effect plots are shown for contralesional SMA-SMC FC contributing to the explanation of variability in follow-up BI, UEFM, MRS and NIHSS in severe stroke patients. There was a significant association between FC SMA-SMC at T1 and BI, UEFM and MRS at T_{2/3} with higher FC values early after stroke found in patients which are likely to show more severe persistent deficits in follow-up. *P* of FC SMA-SMC as the predictors of interests (within-model) is given (uncorrected).

further complicated by a large variability in clinical cohorts, methods and time points investigated. For instance, in well-recovered patients and the chronic stage of recovery, affected hand movements have been linked to an impaired task-related inhibitory information flow from contralesional SMA to contralesional M1¹⁰. In the acute setting, another study observed a reduced inhibitory information flow from SMA to contralesional M1¹¹. An analysis in 81 patients, measured within 2 weeks after ischemic or hemorrhagic stroke, has found a decrease in resting-state FC between contralesional SMA and M1¹². However, none of these studies have reported any coupling-outcome associations. In contrast, one study in severely impaired chronic stroke patients has revealed increased connectivity in the contralesional sensorimotor cortex within the sensorimotor network, when compared to less impaired patients. The level of upregulated contralesional coupling was negatively correlated with the performance of the paretic hand¹³. The present results add to these data by indicating that the upregulation in contralesional connectivity might be an early and specific pattern in severely impaired stroke patients which might also carry, as evidenced for SMA-SMC, relevant information regarding future persistent deficits. As this association was independent of the initial deficit, we argue that the increase in FC might parallel the attempt of the lesioned brain to recruit additional motor cortices of the contralesional hemisphere to support motor functions and facilitate recovery. However, this attempt appears to be largely futile in the end. To what extent an additional contralesional upregulation by means of non-invasive brain stimulation³¹ might help to promote recovery has to be investigated systematically and prospectively in large, well-characterized clinical cohorts. Thereby, models of interhemispheric inhibition suggesting potentially non-beneficial effects in the ipsilesional hemisphere should not stand against these considerations as more recent data have just begun to call those concepts into question³².

Apart from SMA-SMC, FC increases were also present in the contralesional precuneus and cingulate cortices, particularly seeding from M1 and CIPS. These alterations are well in line with previous data obtained in severely impaired acute stroke patients, which also showed an increase in specific states of dynamic FCs between the precuneus and frontal brain regions³³. Chronic stroke patients comparably exhibited a stronger coupling between medial regions of the posterior default mode network and the frontoparietal network³⁴. The absence of significant associations between these alterations and subsequent motor outcome in the present cohort might be explained by the actual focus on the motor domain. Poststroke cognitive impairment and affective symptoms have been associated with FC alterations in default mode network regions^{35,36}.

There are some critical limitations worth noting. First, the authors fully recognize the small sample size in this study, which is likely to reduce the sensitivity and specificity of the present findings. Whole-brain results are corrected for multiplicity in line with the methodological standard. However, subsequent correlations were not corrected for multiple testing, which biases the results towards higher sensitivity at lower specificity. Though, the consistency of SMA-SMC association with multiple outcome scores suggests a specific and valid finding. Nevertheless, these results remain exploratory and preliminary in nature; upcoming studies will have to verify the findings. Second, as outlined in the supplementary material, clinical data of up to six patients were collected after 6 months. Hence, the distribution of the time point of the late subacute stage of recovery might have biased the current findings. In a post-hoc analyses, the significant models summarized by Table 2 were re-evaluated including this additional information as a factor. The analysis revealed, that T_{2/3} had no significant effect. Third, as seed areas, we selected five key areas of the contralesional parieto-frontal motor network. Whether the FC changes might be mediated by hidden, unmodeled nodes remains unclear. Fourth, seed-based FC analyses were computed across the whole brain. However, following our a-priori hypothesis, further statistical analyses were restricted to the contralesional hemisphere as direct lesion effects might be very difficult to quantify and critically influence FC estimates. However, the correction for multiplicity across the brain is still influenced by the ipsilesional hemisphere.

Materials and methods

Cohort and clinical data. The present analyses are based on clinical and imaging data of a previously published prospective cohort study comprising 30 more severely impaired acute stroke patients admitted to the University Medical Center Hamburg-Eppendorf from October 2017 to February 2020⁶. Acute stroke patients (3–14 days after the incident) were included according to the following criteria: first-ever ischemic stroke causing a severe motor deficit involving hand function, modified Rankin Scale (MRS) > 3 or Barthel index (BI) ≤ 30 or 'early rehabilitation' Barthel Index < 30 and age ≥ 18 years. Exclusion criteria were pre-existing clinically silent brain lesions > 1 cm³ or pre-existing motor deficits, contraindications for MRI, relevant psychiatric diseases, drug abuse or pregnancy. A flowchart of study inclusion is given in the original report⁶. Acute stroke patients underwent structural and functional resting-state MRI in the first days after the event as time point T₁ (days 3–14). Follow-up time point T_{2/3} was defined in the late subacute stage of recovery³⁷ after 3 months, or, in patients in which clinical data for this time point was not available, after 6 months. Standardized tests at time point T₁ and T_{2/3} included the BI, the Fugl Meyer Assessment of the upper extremity (UEFM), the MRS, and the National Institutes of Health Stroke Scale (NIHSS). Nineteen Patients were matched with 19 healthy control participants according to age and sex. All patients and controls were right-handed.

Ethics statement. The study was conducted following the Declaration of Helsinki and approved by the local ethics committee of the Medical Association of Hamburg (PV5442). All participants provided informed consent themselves or via a legal guardian, in accordance with the ethical Declaration of Helsinki. All methods were carried out in accordance with relevant guidelines and regulations and all experimental protocols were approved by the Medical Association of Hamburg.

Brain imaging—data acquisition. A 3 T Skyra MRI scanner (Siemens Healthineers, Erlangen, Germany) equipped with a 32-channel head coil were used to acquire multimodal imaging data, including structural high-resolution T1-weighted images and functional resting-state images. For the T1-weighted sequence, a 3-dimensional magnetization-prepared rapid gradient echo (3D-MPRAGE) sequence was used with the following parameters: repetition time (TR) = 2500 ms, echo time (TE) = 2.12 ms, flip angle 9°, 256 coronal slices with a voxel size of 0.8 × 0.8 × 0.9 mm³, field of view (FOV) = 240 mm. The resting-state parameters for blood oxygenation level-dependent (BOLD) contrasts were FOV = 260 mm, TR = 2 s, TE = 30 ms, a 72 × 72 × 32 matrix, voxel size 3 × 3 × 3 mm³, flip angle 90°, and 210 images. Before the resting-state scans, the participants were asked to focus on a black cross located behind the scanner, which could be viewed via a mirror. For analyses, all resting-state and T1-weighted images with right-sided stroke lesions were flipped to the left hemisphere. This hemispheric flip (T1-weighted and fMRI images) was also performed in the controls matched to the patients with right-sided stroke-lesions to account for the distribution of stroke lesions to the dominant and non-dominant hemispheres. This procedure was in line with the original report⁶.

Brain imaging—image analysis. The resting-state images and T1-weighted images were preprocessed using the CONN toolbox v20.b, an SPM12-based toolbox. In line with our previous published work⁶, the default-pipeline for volume-based analysis with the following steps and parameters was used for image pre-processing: The first ten volumes were discarded to account for magnetization equilibrium effects. During the initial pre-processing, all functional images were realigned (motion corrected), centered, slice time corrected, corrected for motion artefacts using the artefact detection tools (ART). All structural and functional images were spatially normalized to MNI space, and the functional images were spatially smoothed to allow for better registration and reduction of noise using a 6 mm full width at half maximum (FWHM) Gaussian kernel. Functional and anatomical data were segmented into grey matter, white matter, and CSF tissue classes using SPM12 unified segmentation and normalization procedure³⁸. After normalization, every image was visually checked for possible registration errors due to the large stroke lesions. After preprocessing, motion parameters were derived from rigid-body realignment and their derivatives. Five potential noise components (average BOLD signal and the first four components in a principle component analysis of the covariance within the subspace orthogonal to the average BOLD signal) derived from cerebrospinal fluid and white matter using the aCompCor (anatomical component based noise correction) procedure, were regressed from the signal^{6,39}. Global signal regression was not included in the analysis to avoid potential false anti-correlations⁴⁰. A temporal band-pass filter between 0.008 and 0.1 Hz was applied to focus on slow-frequency fluctuations while minimizing the influence of physiological, head motion, and other noise sources⁴¹.

Seed-based analysis. In a first level analysis the interregional functional connectivity (FC) was conducted following a whole-brain approach (seed-based analysis) using spherical seeds (radius of 5 mm) for five key areas of the parieto-frontal motor network of the contralesional hemisphere with published MNI coordinates⁹: the primary motor cortex M1 (38, -22, 54), the supplementary motor area SMA (6, -4, 57), the ventral premotor cortex PMV (54, 6, 32), the anterior intraparietal sulcus AIPS (38, -43, 52) and the caudal intraparietal sulcus CIPS (21, -64, 55). Voxel-wise FC values were calculated between these seeds and all other voxels based on Fisher-transformed bivariate cross-correlation coefficients. For group-wise second level, a cluster-based analyses and more precisely Random Field Theory (RFT) parametric statistics⁴² was used to perform the comparison between patients and controls [1 - 1] with a voxel threshold of $P < 0.001$ (uncorrected) and a cluster size threshold of $P < 0.05$ (FDR-corrected). The results were used to identify the peak coordinates of the different clusters and create spherical regions of interest (ROI, radius of 5 mm) around these peak coordinates. The ROIs were used in ROI-to-ROI analyses to obtain individual Fisher-transformed bivariate correlation coefficients (FC) between each pair of seed and peak ROI for further correlational analyses.

Statistical analysis. Statistical analyses were performed in R (version 4.0.4). To assess functional improvement over time, linear-mixed effects models with repeated measures were fitted with TIME as the factor of interest and ID as random effect. If available, the 3 months follow-up time point was used, otherwise clinical data after 6 months were used in line with the original work⁶. To assess FC-outcome relationships, individual linear models were constructed with follow-up BI, UEFM, MRS or NIHSS as dependent variable and cluster-wise FC value as the predictor of interest and the initial deficit at T₁ (equivalent score) and AGE as covariates to adjust the target effects. Model results are presented by predictor coefficients with their significances and overall explained variance of the final models. Statistical significance was set to a $P < 0.05$ (uncorrected).

Data availability

Data will be made available upon reasonable request to the corresponding author, which includes submitting an analysis plan for a secondary project.

Received: 11 March 2023; Accepted: 2 July 2023

Published online: 07 July 2023

References

1. Rehme, A. K. & Grefkes, C. Cerebral network disorders after stroke: Evidence from imaging-based connectivity analyses of active and resting brain states in humans. *J. Physiol.* **591**, 17–31. <https://doi.org/10.1113/jphysiol.2012.243469> (2012).
2. Wang, L. *et al.* Dynamic functional reorganization of the motor execution network after stroke. *Brain A J. Neurol.* **133**, 1224–1238 (2010).
3. Park, C. H. *et al.* Longitudinal changes of resting-state functional connectivity during motor recovery after stroke. *Stroke A J. Cereb. Circ.* **42**, 1357–1362 (2011).
4. Chen, J. L. & Schlaug, G. Resting state interhemispheric motor connectivity and white matter integrity correlate with motor impairment in chronic stroke. *Front. Neurol.* **4**, 178 (2013).
5. Frías, I. *et al.* Interhemispheric connectivity of primary sensory cortex is associated with motor impairment after stroke. *Sci. Rep.* **8**, 12601 (2018).
6. Backhaus, W., Braaß, H., Higgen, F. L., Gerloff, C. & Schulz, R. Early parietofrontal network upregulation relates to future persistent deficits after severe stroke—A prospective cohort study. *Brain Commun.* **3**, 1–10 (2021).
7. Paul, T. *et al.* Early motor network connectivity after stroke: An interplay of general reorganization and state-specific compensation. *Hum. Brain Mapp.* **42**, 5230–5243 (2021).
8. Bönstrup, M. *et al.* Clinical parietofrontal network upregulation after motor stroke. *NeuroImage. Clin.* **18**, 720–729 (2018).
9. Schulz, R. *et al.* Enhanced effective connectivity between primary motor cortex and intraparietal sulcus in well-recovered stroke patients. *Stroke* **47**, 482–489 (2016).
10. Binder, E. *et al.* Cortical reorganization after motor stroke: A pilot study on differences between the upper and lower limbs. *Hum. Brain Mapp.* **42**, 1013–1033 (2021).
11. Rehme, A. K., Eickhoff, S. B., Wang, L. E., Fink, G. R. & Grefkes, C. Dynamic causal modeling of cortical activity from the acute to the chronic stage after stroke. *Neuroimage* **55**, 1147–1158 (2011).
12. Lee, J. *et al.* Alteration and role of interhemispheric and intrahemispheric connectivity in motor network after stroke. *Brain Topogr.* **31**, 708–719 (2018).
13. Hong, W. *et al.* Diverse functional connectivity patterns of resting-state brain networks associated with good and poor hand outcomes following stroke. *NeuroImage Clin.* **24**, 102065 (2019).
14. Siegel, J. S. *et al.* Re-emergence of modular brain networks in stroke recovery. *Cortex* **101**, 44–59 (2018).
15. Gratton, C., Nomura, E. M., Pérez, F. & D'Esposito, M. Focal brain lesions to critical locations cause widespread disruption of the modular organization of the brain. *J. Cogn. Neurosci.* **24**, 1275 (2012).
16. Favre, I. *et al.* Upper limb recovery after stroke is associated with ipsilesional primary motor cortical activity: A meta-analysis. *Stroke* <https://doi.org/10.1161/STROKEAHA.113.003168> (2014).
17. Rehme, A. K., Eickhoff, S. B., Rottschy, C., Fink, G. R. & Grefkes, C. Activation likelihood estimation meta-analysis of motor-related neural activity after stroke. *Neuroimage* **59**, 2771–2782 (2012).
18. Koch, P. J. & Hummel, F. C. Toward precision medicine: Tailoring interventional strategies based on noninvasive brain stimulation for motor recovery after stroke. *Curr. Opin. Neurol.* **30**, 388–397 (2017).
19. Liu, H., Cai, W., Xu, L., Li, W. & Qin, W. Differential reorganization of SMA subregions after stroke: A subregional level resting-state functional connectivity study. *Front. Hum. Neurosci.* **13**, 468 (2020).
20. Brodtmann, A. *et al.* Changes in regional brain volume 3 months after stroke. *J. Neurol. Sci.* **322**, 122–128 (2012).
21. Rojas Albert, A. *et al.* Cortical thickness of contralesional cortices positively relates to future outcome after severe stroke. *Cereb. Cortex* <https://doi.org/10.1093/CERCOR/BHAC040> (2022).
22. Johansen-Berg, H. *et al.* The role of ipsilateral premotor cortex in hand movement after stroke. *Proc. Natl. Acad. Sci. U. S. A.* **99**, 14518–14523 (2002).
23. Lotze, M. *et al.* The role of multiple contralesional motor areas for complex hand movements after internal capsular lesion. *J. Neurosci.* **26**, 6096–6102 (2006).
24. Volz, L. J. *et al.* Time-dependent functional role of the contralesional motor cortex after stroke. *NeuroImage Clin.* **16**, 165–174 (2017).
25. Schönle, P. D. Frühreha-barthelindex (FRB) - eine frührehabilitationsorientierte erweiterung des barthelindex. *Rehabilitation* **34**, 69–73 (1995).
26. Rehme, A. K., Fink, G. R., Von Cramon, D. Y. & Grefkes, C. The role of the contralesional motor cortex for motor recovery in the early days after stroke assessed with longitudinal fMRI. *Cereb. Cortex* **21**, 756–768 (2011).
27. Gerloff, C. *et al.* Multimodal imaging of brain reorganization in motor areas of the contralesional hemisphere of well recovered patients after capsular stroke. *Brain* **129**, 791–808 (2006).
28. Schaechter, J. D. & Perdue, K. L. Enhanced cortical activation in the contralesional hemisphere of chronic stroke patients in response to motor skill challenge. *Cereb. Cortex* **18**, 638–647 (2008).
29. Ward, N., Brown, M., Thompson, A. & Frackowiak, R. Neural correlates of outcome after stroke: A cross-sectional fMRI study. *Brain* **126**, 1430–1448 (2003).
30. Calautti, C. *et al.* The relationship between motor deficit and hemisphere activation balance after stroke: A 3T fMRI study. *Neuroimage* **34**, 322–331 (2007).
31. Schulz, R., Gerloff, C. & Hummel, F. C. Non-invasive brain stimulation in neurological diseases. *Neuropharmacology* **64**, 579–587 (2013).
32. Xu, J. *et al.* Rethinking interhemispheric imbalance as a target for stroke neurorehabilitation. *Ann. Neurol.* **85**, 502–513 (2019).

33. Bonkhoff, A. K. *et al.* Abnormal dynamic functional connectivity is linked to recovery after acute ischemic stroke. *Hum. Brain Mapp.* **42**, 2278–2291 (2021).
34. Zhao, Z. *et al.* Altered intra- and inter-network functional coupling of resting-state networks associated with motor dysfunction in stroke. *Hum. Brain Mapp.* **39**, 3388–3397 (2018).
35. Ding, X. *et al.* Patterns in default-mode network connectivity for determining outcomes in cognitive function in acute stroke patients. *Neuroscience* **277**, 637–646 (2014).
36. Lassalle-Lagadec, S. *et al.* Subacute default mode network dysfunction in the prediction of post-stroke depression severity. *Radiology* **264**, 218–224 (2012).
37. Bernhardt, J. *et al.* Agreed definitions and a shared vision for new standards in stroke recovery research: The stroke recovery and rehabilitation roundtable taskforce. *Neurorehabil. Neural Repair* **31**, 793–799 (2017).
38. Ashburner, J. & Friston, K. J. Unified segmentation. *Neuroimage* **26**, 839–851 (2005).
39. Behzadi, Y., Restom, K., Liao, J. & Liu, T. T. A component based noise correction method (CompCor) for BOLD and perfusion based fMRI. *Neuroimage* **37**, 90–101 (2007).
40. Murphy, K., Birn, R. M., Handwerker, D. A., Jones, T. B. & Bandettini, P. A. The impact of global signal regression on resting state correlations: Are anti-correlated networks introduced?. *Neuroimage* **44**, 893–905 (2009).
41. Hallquist, M. N., Hwang, K. & Luna, B. The nuisance of nuisance regression: Spectral misspecification in a common approach to resting-state fMRI preprocessing reintroduces noise and obscures functional connectivity. *Neuroimage* **82**, 208–225 (2013).
42. Worsley, K. J. *et al.* A unified statistical approach for determining significant signals in images of cerebral activation. *Hum. Brain Mapp.* **4**, 58–73 (1996).

Author contributions

Study Design: R.S., W.B. Data acquisition: W.B., F.H. Data analysis and statistical analysis: H.B., L.G., R.S. Data interpretation: H.B., L.G., F.H., R.S., F.Q., C.U.C., C.G. First Manuscript: H.B., L.G. All authors reviewed the manuscript.

Funding

Open Access funding enabled and organized by Projekt DEAL. This work was funded by the Deutsche Forschungsgemeinschaft (DFG, German Research Foundation) SFB 936-178316478—Project C1 to C.G.), the DFG in cooperation with the National Science Foundation of China (NSFC) (SFB TRR-169/A3 to C.G.) and the Else Kröner-Fresenius-Stiftung (2016_A214 to R.S.). R.S. and C.U.C. are additionally supported by an Else Kröner Exzellenzstipendium from the Else Kröner-Fresenius-Stiftung (2020_EKES.16 to R.S., 2018_EKES.04 to C.U.C.). F.Q. is supported by the Gemeinnützige Hertie-Stiftung (Hertie Network of Excellence in Clinical Neuroscience).

Competing interests

The authors declare no competing interests.

Additional information

Supplementary Information The online version contains supplementary material available at <https://doi.org/10.1038/s41598-023-38066-0>.

Correspondence and requests for materials should be addressed to H.B.

Reprints and permissions information is available at www.nature.com/reprints.

Publisher's note Springer Nature remains neutral with regard to jurisdictional claims in published maps and institutional affiliations.



Open Access This article is licensed under a Creative Commons Attribution 4.0 International License, which permits use, sharing, adaptation, distribution and reproduction in any medium or format, as long as you give appropriate credit to the original author(s) and the source, provide a link to the Creative Commons licence, and indicate if changes were made. The images or other third party material in this article are included in the article's Creative Commons licence, unless indicated otherwise in a credit line to the material. If material is not included in the article's Creative Commons licence and your intended use is not permitted by statutory regulation or exceeds the permitted use, you will need to obtain permission directly from the copyright holder. To view a copy of this licence, visit <http://creativecommons.org/licenses/by/4.0/>.

© The Author(s) 2023